

Circular Polarization of Circumstellar Water Masers around S Per

W. Vlemmings¹, P.J. Diamond², and H.J. van Langevelde³

¹ Sterrewacht Leiden, Postbus 9513, 2300 RA Leiden, the Netherlands

² Jodrell Bank Observatory, University of Manchester, Macclesfield, Cheshire, SK11 9DL, England

³ Joint Institute for VLBI in Europe, Postbus 2, 7990 AA Dwingeloo, The Netherlands

Received ; accepted

Abstract. We present the first circular polarization measurements of circumstellar H₂O masers. Previously the magnetic field in circumstellar envelopes has been estimated using polarization observations of SiO and OH masers. SiO masers are probes of the high temperature and density regime close to the central star. OH masers are found at much lower densities and temperatures, generally much further out in the circumstellar envelope. The detection of the circular polarization of the (6₁₆–5₂₃) rotational transition of the H₂O maser could be attributed to Zeeman splitting due to the magnetic field in the intermediate temperature and density regime. The fields inferred here agree well with predicted values for a combination of the r^{-2} dependence of a solar-type magnetic field, and the coupling of the field to the high density masing regions. We also discuss the unexpected narrowing of the circular polarization spectrum.

formation is available. In this region the H₂O maser emission occurs. Since water is a non-paramagnetic molecule, determination of the magnetic field is significantly more difficult. The Zeeman splitting of H₂O is extremely small for the field strengths expected (few hundred mG), only $\approx 10^{-3}$ times the typical Gaussian line width of the H₂O maser line ($\Delta\nu_L \approx 20$ kHz). However, Fiebig & Güsten (1989, hereafter FG) showed that in the presence of such magnetic fields the Zeeman splitting can be detected with high spectral resolution polarization observations. Their observations targeted strong interstellar H₂O maser features. The observations presented here give the first results of circular polarization measurements of the H₂O masers found in CSEs. We have used a method similar to that used in FG to determine the magnetic field strength parallel to the line of sight. Like FG we are limiting ourselves to a Zeeman interpretation of the observed splitting, although a non-Zeeman interpretation has been presented in Neduloha & Watson (1990).

1. Introduction

High mass loss in late type stars produces a circumstellar envelope (CSE) in which several different maser species can be found. These masers, especially SiO, H₂O and OH, are excellent tracers of the dynamics and kinematics of the CSEs. Polarization observations of these masers have revealed the strength and structure of the magnetic field throughout the CSE. Observations of SiO maser polarization have shown highly ordered magnetic fields close to the central star, at radii of 5-10 AU where the SiO maser emission occurs (Kemball & Diamond, 1997). The standard Zeeman interpretation gives magnetic field strengths of ≈ 5 -10 G. However, a non-Zeeman interpretation has been proposed by Wiebe & Watson (1998), which only requires fields of ≈ 30 mG. At much lower densities and temperatures and generally much further from the star, OH maser observations measure fields of ≈ 1 mG (Szymczak & Cohen, 1997; Masheder et al., 1999). But for the intermediate region, at distances of a few hundred AU, no in-

2. Observations

The observations were performed at the NRAO¹ Very Long baseline Array (VLBA) in December 1998. We observed 4 late type stars (S Per, U Her, VY CMa and NML Cyg), the results presented here are the first results for the supergiant S Per, the source with strong water maser features and relatively simple structure. The stellar velocity V_{LSR} of S Per is -38.5 km s⁻¹. The beam width at 22.235 GHz, the frequency of the 6₁₆ – 5₂₃ rotational transition of H₂O, is $\approx 0.7 \times 0.3$ mas. This allows us to resolve the different H₂O maser features in the CSE. The data were correlated twice, once with modest (7.8 kHz = 0.1 km s⁻¹) spectral resolution, which enabled us to generate all 4 polarization combinations (RR, LL, RL and LR). The second correlator run was performed with high spectral resolution (1.95 kHz = 0.027 km s⁻¹), necessary to detect the circular polarization signature of the H₂O Zeeman splitting,

¹ The National Radio Astronomy Observatory is a facility of the National Science Foundation operated under cooperative agreement by Associated Universities, Inc.

and therefore only contained the two polarization combinations RR and LL. The data produced by the first correlator run were used to accurately calibrate the R- and L-polarization. The calibration solutions were obtained on R and applied to L after we determined the relative R-L corrections, assuming the R- and L-polarization line profiles to be similar. The solutions were then applied to the dataset produced by the second correlator run, which we used to determine the circular polarization V for the separate maser features. The data analysis followed the method of Kemball, Diamond & Cotton (1995).

3. Background

The H_2O ($6_{16} - 5_{23}$) rotational transition consists of 6 hyperfine components. Analyses of interstellar water masers indicate that all 6 hyperfine components contribute to the maser (Walker, 1984). The observed intensity ratios however, frequently deviate from those obtained from molecular transition probabilities (Moran et al., 1973; Genzel et al., 1979). Our analysis is performed using fitted line ratios for the 3 strongest hyperfine components ($F = 7 - 6$, $6 - 5$ and $5 - 4$). The separation between these components is 0.45 and 0.58 km s^{-1} respectively. The weakest components ($F = 5 - 6$, $5 - 5$ and $6 - 6$) are separated by more than 2.5 km s^{-1} . They are not observed in the total power spectrum so we have not included them in our analysis. Our treatment follows closely the analysis performed in FG. Here we have added the possibility of multiple masering hyperfine components. We assume the strongest hyperfine component ($F = 7 - 6$) to be the dominant transition. Because of the non-paramagnetic nature of the H_2O molecule, the Zeeman splitting is extremely small. It is due to the interaction of the nuclear magnetic moment with the external B field. Thus the splitting is a factor of 10^3 weaker than that for radicals like OH. In the weak field limit, the split energy ΔE_Z of a given energy level (J, F, I) is determined by:

$$\Delta E_Z = -\{\alpha_J g_J + \alpha_I g_I\} \cdot \mu_N M_F \cdot B_{\text{Gauss}} \quad (1)$$

with :

$$\alpha_J = \{J(J+1) + F(F+1) - I(I+1)\}/2F(F+1),$$

$$\alpha_I = \{F(F+1) + I(I+1) - J(J+1)\}/2F(F+1).$$

This corresponds to a characteristic frequency shift of the order of $\Delta\nu_Z \approx 10^3 \text{ Hz} \cdot [B_{\text{Gauss}}]$. Where $I(= 1)$ is the nuclear spin, μ_N the nuclear magneton and M_F the magnetic quantum number; $g_I = 5.585$, and the g_J -factors $g_6 = 0.6565$ and $g_5 = 0.6959$ are from Kukolich (1969).

Each hyperfine component will split into 3 groups of lines (σ^+ , σ^- and π), as seen in Fig. 1 for one of the hyperfine components. The relative strengths of the transition probabilities have been determined by Deguchi & Watson (1986). For a magnetic field B parallel to the line of sight the Zeeman pattern consists of the two circular polarized σ components only. The right- and left-handed (RR and LL)

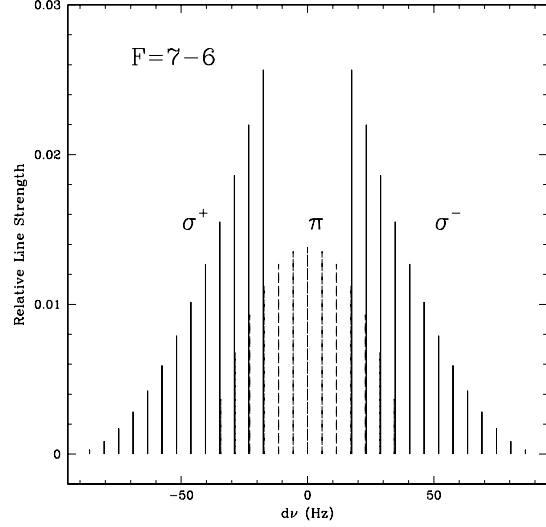


Fig. 1. The Zeeman pattern of the $F = 7 - 6$ hyperfine component for an external field of 50 mG .

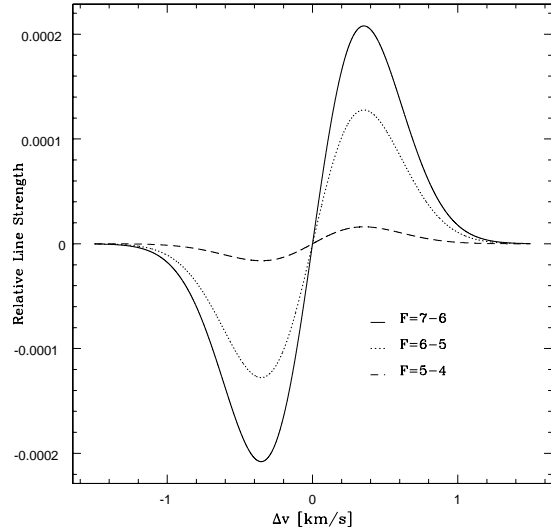


Fig. 2. Synthetic V-spectra for $F = 7 - 6$, $6 - 5$ and $5 - 4$ calculated for an external field of 50 mG and a line width of $\Delta\nu_L = 0.5 \text{ km s}^{-1}$.

spectra, corresponding to the σ^\pm components will only be slightly shifted against each other ($\Delta\nu_Z \approx 10^{-3}$ to -4 times $\Delta\nu_L$). As a result, the observed V-spectrum (RR-LL) will be a sine-shaped function, corresponding to the derivative I' of the total power spectrum. The amplitude of this function depends on the maser line width, the magnetic field strength, and on which hyperfine components actually contribute to the maser. By calculating synthetic V-spectra from the Zeeman pattern for different line widths, magnetic field strength and hyperfine combi-

nations we find the following relation for the percentage of circular polarization:

$$P_V \equiv (V_{\max} - V_{\min})/I_{\max} = A_{F-F'} \cdot B_{\text{Gauss}}/\Delta v_L. \quad (2)$$

Here V_{\max} and V_{\min} are the maximum and minimum of the synthetic V-spectrum fitted to the observations. Δv_L [km s⁻¹] is the Gaussian line width of the total power spectrum, and I_{\max} is the peak flux of the maser feature. B is the magnetic field component along the line of sight. The $A_{F-F'}$ [·10⁻³] coefficient depends on the masering hyperfine components. The $A_{F-F'}$ coefficients have been determined by calculating P_V from synthetic V-spectra, determined for a series of magnetic field strengths B , and for the different hyperfine components. For the $F = 7-6$, $6-5$ and $5-4$ components individually we find $A_{F-F'} = 16.22, 10.00$ and 1.23 respectively. For a fitted combination of hyperfine components we find slightly different values. An example of synthetic V-spectra for the three hyperfine lines is shown in Fig. 2.

However, due to the complex interactions between the various hyperfine components in the maser regime, deviations from the V-spectrum proportionality are possible. Detailed radiative transfer treatment, as performed by Nedoluha & Watson (1992; hereafter NW), for instance, resulted in $A_{F-F'} = 23.9$.

4. Results

Fig. 3 shows the total intensity map of the water maser features surrounding S Per. We are able to identify most of the maser features detected in earlier observations (Diamond et al., 1987; Marvel, 1997). The positions are relative to the brightest maser feature, for which we have managed to determine the circular polarization spectrum shown in Fig 4. This figure also shows a χ^2 -fit to the sine-shape spectrum. The amplitude of the V-spectrum is only a small fraction ($\approx 1\%$) of the total power, so we have only been able to determine the Zeeman splitting, and thus magnetic field strength, for the brightest maser feature. We do not detect circular polarization in any of the other bright maser features although, if it was present at the same absolute level as in the brightest feature, we would have detected it. This further confirms our detection, because a scaled down version of the total power I would also have been detectable on the other strong features if calibration errors were significant.

The total power spectrum indicates that one of the hyperfine components clearly dominates, since the splitting of the hyperfine lines should otherwise have been observable. We have performed a fit to the total power spectrum to determine the maser line width and the best fitted ratio for the three strongest hyperfine transitions. Using this line ratio we have calculated the $A_{F-F'}$ coefficient as described above. In this case we find $A_{F-F'} = 15.54$. Using the fitted Gaussian line width ($\Delta v_L = 0.44 \pm 0.01$ km s⁻¹) and $P_V = (9.9 \pm 0.5) \cdot 10^{-3}$ in Eq. 2, we find

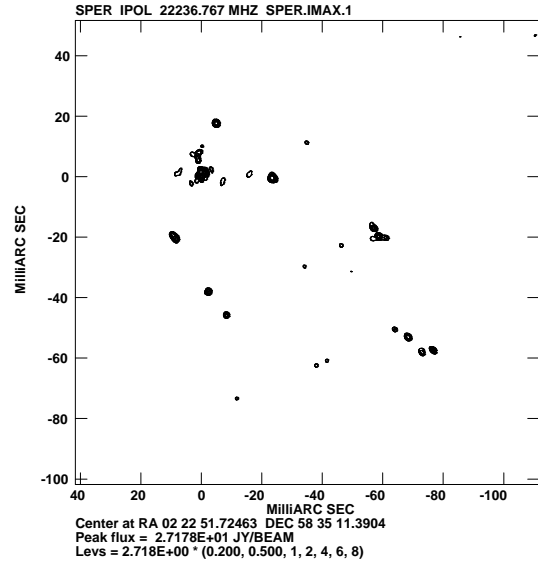


Fig. 3. Total intensity image of the H₂O maser features around S Per.

for the magnetic field strength along the line of sight $B_{||} = 279 \pm 30$ mG. If only the $F = 7-6$, $6-5$ or $5-4$ hyperfine transition contributes the magnetic field should be scaled by 0.96, 1.55 or 12.63 respectively. As seen in Fig. 4 the V-spectrum is negative on the blue shifted side, therefore the observed component $B_{||}$ is pointing away from us. This result is the first measured circular polarization in the circumstellar water maser region.

5. Discussion

As discussed above, the magnetic field strength was obtained by using a best fitted line ratio for the three main hyperfine components. A radiative transfer treatment for the polarized maser radiation of the $6_{16} - 5_{23}$ H₂O rotational transition was performed by NW. Some difficulties exist matching their results to our observations of the total intensity spectrum, which shows an almost Gaussian shape. Their treatment also did not predict the anti-symmetric shape of the V-spectrum as shown in our observations and those by FG. However, since the calibration performed here and by FG assumes similar R- and L-polarization line profiles, the anti-symmetric shape is a necessary result of the treatment of the data.

The observed V-spectrum however, is not directly proportional to I' either, as would have been expected in the simple model. The minimum and maximum of the sine-shaped function are not located at $\pm\sigma/\sqrt{2}$, with σ being the observed Gaussian line width. Instead they are found at $\Delta\nu$ smaller by a factor of ≈ 2.5 with respect to the line width fitted to the total power spectrum. Possibly, this narrowing of the V-spectrum can be attributed to the overlap of the multiple hyperfine components, as predicted by the treatment and analysis of NW. The observed

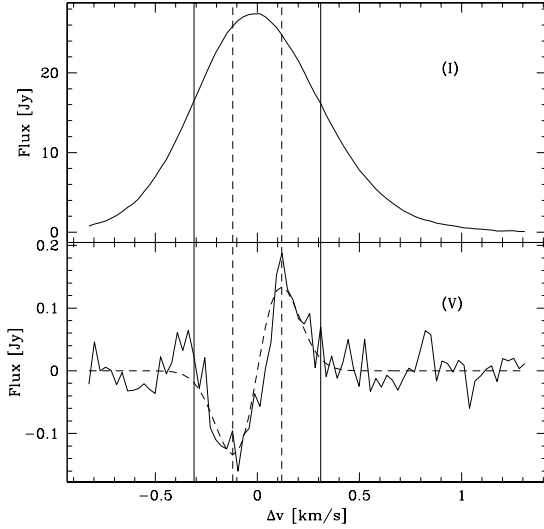


Fig. 4. Total power (I) and circular polarization (V) spectrum of the brightest H_2O maser feature around S Per. The dashed line is the fit of the synthetic V -spectrum to the observed spectrum. Also shown are the observed (dashed) and expected (solid) positions of the minimum and maximum of the V -spectrum.

effect, however, still seems too large. Due to this our magnetic field strength could be overestimated by at most a factor of 2. The interstellar water masers observed by FG did not show this narrowing.

Because of the narrowing of the V -spectrum it is difficult to address the saturation state of the maser. Elitzur (1998) showed that the observed circular polarization spectrum would be a good indication of the maser saturation state. If the ratio of $V(\nu)/I(\nu)$ increased towards the wings of the line instead of showing a constant ratio the maser is thought to be unsaturated. This is however, almost the opposite effect of what we observe. Until the narrowing of the circular polarization is fully explained our observations are difficult to reconcile with a specific saturation state.

We have also tried to determine the linear polarization of the maser features around S Per, but no indication of linear polarization has been found. This is consistent with the observations of Barvainis & Deguchi (1989). They explain that the absence of linear polarization is probably due to the fact that masers are not very strongly saturated, and that infrared radiation does not contribute significantly to the pumping process.

The magnetic field strength derived this way is within the range estimated by previous observations of SiO and OH masers. As noted before, polarization observations of SiO masers close to the central star reveal fields of 5-10 G, assuming a standard Zeeman interpretation. OH maser observations of features around S Per indicate a field of slightly less than 1 mG (Masheder et al., 1999). Based on

these values, the dependence of $B \propto r^{-2}$ for a solar-type magnetic field is the most likely. For a dipole medium, the magnetic field is expected to vary with r^{-3} , which appears to be too steep to accurately describe the observations.

In S Per, the H_2O and OH masers are observed to exist at similar *projected* distances (Masheder et al., 1999). This would disagree with the observed differences in the magnetic field strengths, except if the magnetic field could remain frozen in high density clumps. The magnetic field strength is then expected to vary with number density as $B \propto n^k$, with $1/3 \leq k \leq 1/2$ from theoretical predictions (e.g Mouschovias 1987), where n is the number density. SiO masers are observed in high density clumps at 5 – 10 AU from the central star. H_2O masers exist in similar clumps at distances of a few hundred AU, with the magnetic field lines frozen in the dense medium. Richards et al. (1999) show that the OH and H_2O maser clumps avoid each other, although located at similar projected distances. They conclude that the density ratio between the H_2O maser clumps and the OH in the surrounding medium only needs to be a factor of 50. However, magnetic fields frozen into the maser clumps would require a density ratio of $\approx 10^4$ to explain the difference in field. This seems to indicate that actual coexistence between the OH and H_2O masers is unlikely.

In conclusion, although the exact influence of the hyperfine interaction is not yet clear, we derive a magnetic field strength of $B_{\parallel} = 279 \pm 30$ mG.

Acknowledgments: This project is supported by NWO grant 614-21-007.

References

- Barvainis, R., Deguchi, S., 1989, AJ, 97, 1089.
- Deguchi, S., Watson, W.D., 1986, ApJ, 302, 750.
- Diamond, P.J., et al., 1987, AA, 174, 95.
- Elitzur, M., 1998, ApJ, 504, 390.
- Fiebig, D., Güsten, R., 1989, AA, 214, 333.
- Genzel, R., et al., 1979, AA, 78, 239.
- Kemball, A.J., Diamond, P.J., Cotton, W.D., 1995, A&AS, 110, 383.
- Kemball, A.J., Diamond, P.J., 1997, ApJ, 481, L111.
- Kukolich, S.G., 1969, J. Chem. Phys., 50, 3751.
- Marvel, K., 1997, Ph.D Thesis, new Mexico State University.
- Masheder, M.R.W., Van Langevelde, H.J., Richards, A.M.S., Greenhill, L., Gray, M.D., 1999, NewAR, 43, 563.
- Moran, J.M., et al., 1973, ApJ, 185, 535.
- Mouschovias, T.Ch, 1987, Physical Processes in Interstellar Clouds, eds. G.E. Morfill, M. Scholer, Reidel, Dordrecht, p.453.
- Nedoluha, G.E., Watson, W.D., 1990, ApJ, 361, L53.
- Nedoluha, G.E., Watson, W.D., 1992, ApJ, 384, 185.
- Richards, A.M.S., Yates, J.A., Cohen, R.J., 1999, MNRAS, 306, 954.
- Szymczak, M., Cohen, R.J., 1997, MNRAS, 288, 945.
- Walker, R.C., 1984, ApJ, 280, 618.
- Wiebe, D.S., Watson, W.D., 1998, ApJ, 503, L71.